Nationaal Lucht- en Ruimtevaartlaboratorium
National Aerospace Laboratory NLR

NLR-TP-2001-632

Flap noise measurements in a closed wind tunnel with a phased array

H.M.M. van der Wal and P. Sijtsma

Nationaal Lucht- en Ruimtevaartlaboratorium
National Aerospace Laboratory NLR

NLR-TP-2001-632

Flap noise measurements in a closed wind tunnel with a phased array

H.M.M. van der Wal and P. Sijtsma

The contents of this report have been initially prepared for publication as AIAA paper 2001-2170 in the proceedings of the 7th AIAA-CEAS Aeroacoustics Conference, Maastricht, The Netherlands on 28-30 May, 2001.

Division:	Fluid Dynamics
Issued:	28 December 2001
Classification of title:	Unclassified

Contents

Nomenclature 3

I. Introduction 3

II. Test set-up and experimental methods 4
General 4
Aircraft model 4
Wind tunnel 6
Acoustic array 6
Reference source 6
Test conditions and measuring program 7

III. Experimental results 9
Aircraft model 9
Reference source 11

IV. Conclusions 12
References 13

14 Figures

(13 pages in total)

FLAP NOISE MEASUREMENTS IN A CLOSED WIND TUNNEL WITH A PHASED ARRAY

Henk van der Wal [*], Pieter Sijtsma[†]
National Aerospace Laboratory NLR, 8300 AD Emmeloord, The Netherlands

The effects of winglet type "fences" at the outboard flap tip, and a blunt flap trailing edge on the airframe noise have been measured in a low-speed wind tunnel on a 8.5% half model. Both a single (extending downward) and a double type "fence" configuration (extending upward as well as downward from the wing) have been investigated. An airframe noise reduction up to 7 dB has been found for the flap tip source, which was about equal for the single and double fence configurations. For the blunt trailing edge no significant airframe noise effects were found.
Reflections of the sound waves at the wind tunnel walls may cause errors in the measured airframe noise sound powers. Sound absorbing tunnel wall linings may reduce these errors. From measurements with a reference source, it was found that these errors are small for the present test setup and the frequency range of 4 kHz and higher, which was relevant for the present measurements. It was also found that an absorbing tunnel wall has little effect on the measured source strengths, both for the aircraft model and the reference source, which supports the conclusion of small errors due to tunnel wall reflections.

Nomenclature

a = nozzle radius (3.5mm) [m], Eq. (1)
a_n = neck radius (1mm) [m], Eq. (3)
C_L = wing lift coefficient [-]
c = speed of sound [m/s], Eq. (3)
f_{max} = upper frequency [Hz]
k = wavenumber [m^{-1}], Eq. (1)
L = neck length (1.5mm) [m], Eq. (3)
p = sound pressure [Pa], Eq. (1)
p_H = sound pressure [Pa], Eq. (2)
p_N = sound pressure in the nozzle [Pa], Eq. (1)
R = normalized specific resistance [-], Eq. (2)
r = distance from the nozzle [m], Eq. (1)
S = nozzle cross sectional surface [m^2], Eq. (1)
S_n = neck cross sectional surface [m^2], Eq. (4)
SPL = sound pressure level [dB re 20 μPa]
V = resonator volume (142mm^3) [m^3], Eq. (3)
X = normalized specific reactance [-], Eq. (2)
x = axial tunnel coordinate [m]
y = lateral tunnel coordinate [m]
z = vertical tunnel coordinate [m]
Δ = reference microphone position [m], Eq. (1)
ν = kinematic viscosity of air [m^2/s], Eq. (3)
ω = radial frequency [s^{-1}], Eq. (3)

I. Introduction

Many years of aero-acoustic research have yielded a major noise reduction for propulsion systems of commercial aircraft. For modern turbofan aircraft the engines are no longer the dominating source of aircraft noise, in particular during approach. Triggered by the increasing flows of air traffic, the airport noise regulations follow the noise abatement technology (or is it the other way round?). Anyhow, to comply with the more stringent noise legislation in the future, airframe noise has to be taken into account in the design process of new commercial aeroplanes. Flap side-edge noise is one of the significant contributors to airframe noise[1], for which analysis tools[2,3] and noise reducing measures[4,5,6] are under investigation.

The rapid development of phased arrays during recent years has added a powerful tool in the wind tunnel

[*]Research Engineer, Aeroacoustics Department, P.O. Box 153, e-mail: vdwal@nlr.nl.
[†]Research Engineer, Aeroacoustics Department, P.O. Box 153, e-mail: sijtsma@nlr.nl.

analysis of the farfield airframe noise characteristics[1,7,8,9]. Until a few years ago, acoustic farfield measurements in closed-circuit wind tunnels found very limited application, because of multiple tunnel wall reflections, interfering noise sources related to the wind tunnel propulsion system and pressure fluctuations in the turbulent boundary layer. Recently, both NLR and DNW have acquired an identical 128 channel system for the acquisition and processing of acoustic data. With this system, it is possible to perform acoustic measurements up to 100 kHz, virtually without limitations on the measurement time[10]. Both systems can easily be coupled and extended further without loss of performance. This increases highly the capability for phased array measurements on wind tunnel models.

Besides low-noise characteristics, an adequate aerodynamic performance (lift/drag ratio) is required for high lift devices. Another part of the aerodynamic characteristics of high lift devices is the effect on the wake vortex, which is particularly important for very large aircraft like the Airbus A380. The required minimum distance between successive aeroplanes during approach, and thus the airport capacity, is determined by these vortices.

The upper considerations led NLR to perform an exploratory study, both on the aerodynamic and aero-acoustic effects of a flap tip fence[11]. The study has been financed by own NLR funds. The present paper presents only the aero-acoustic results. The aerodynamic results will be published later.

II. Test set-up and experimental methods

General

As a first test with the new acquisition system an experiment on a 8.5% half model in landing configuration has been performed in the DNW-LST closed-circuit 2.25m×3m wind tunnel (Fig. 1). In particular the effects of flap tip fences and a blunt flap trailing edge on the emission of airframe noise have been investigated. For this experiment a 96 microphone phased array system was mounted flush in the wind tunnel sidewall at the pressure side of the wing (red support plate, Fig. 1).

Due to reflections of the sound waves at the wind tunnel walls, the measured values of the sound powers of the airframe noise sources on the model may deviate from the true values. To obtain an impression of the differences between the measured and true values, also measurements have been carried out with a reference source (Fig. 2), with a known volume velocity. The effect of sound absorbing lining of the tunnel walls on these differences has also been determined.

Fig. 1 Aircraft model and acoustic array in the DNW-LST test section

Fig. 2 Reference source with monopole sound radiation

Aircraft model

The wind tunnel model used in this study was a half-fuselage with a port wing but without tail planes and without pylon/nacelle. The main dimensions are: (semi-)span 1.45m, fuselage length 2.7m, fuselage (half) diameter 0.34 m. In the past, this model has been used extensively by the former Fokker Aircraft

Company for high-lift configuration studies. Fig. 1 presents a picture of this model as mounted in the wind tunnel.

The model can be equipped with several different high-lift device configurations. For the present investigation it was tested in the configuration with leading-edge slat retracted but with the trailing-edge flaps extended (Fig. 3).

Fig. 3 Aircraft model view from wing pressure side ("clean" landing configuration)

The dimensions of the flap tip fence (Fig. 4) are based on both aerodynamic and aero-acoustic design considerations. It was decided to partition the upper and lower parts of the fence so that they could be tested separately as well as in combination. Fig. 5 shows the situation with only the lower fence mounted as seen from two different directions. Behind the fence the wing flap is visible, deflected for the landing configuration. The gap between flap and (lower) fence was sealed by special inserts and/or plasticine (shown in red in Fig. 4 and Fig. 5). For the blunt trailing edge only aerodynamic design criteria have been considered. The blunt flap trailing edge was about three times as thick as the standard trailing edge.

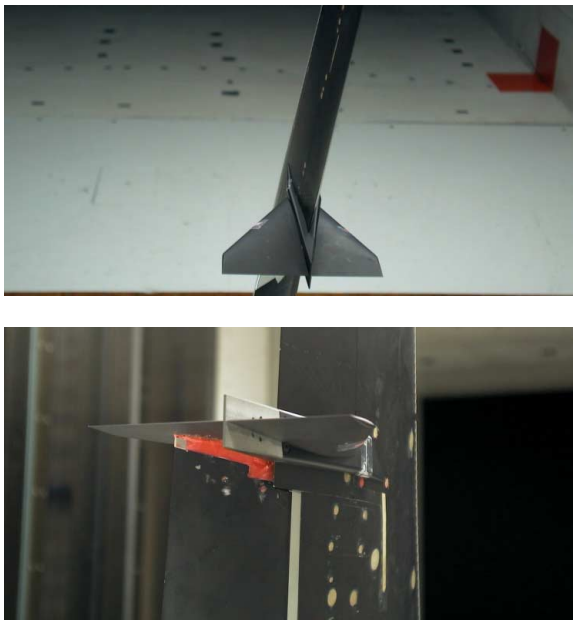

Fig. 4 Details of the flap tip fence (upper plus lower fence) on the aircraft model (flaps removed on upper photo)

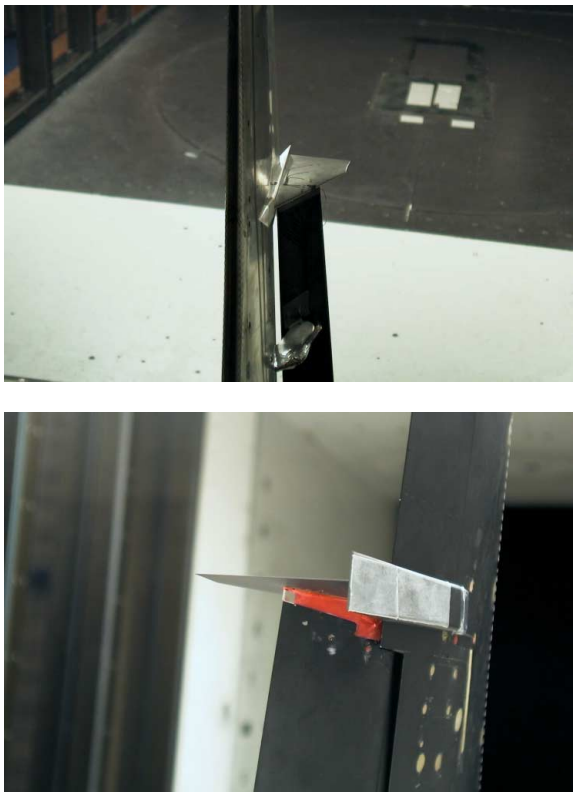

Fig. 5 Details of the flap tip fence (lower fence only) mounted on the aircraft model in landing configuration

Wind tunnel
The tests were done in the DNW-LST, a low-speed, closed circuit type atmospheric wind tunnel with a contraction ratio of 9 and a maximum velocity of 80m/s. The dimensions of the test section are: width 3.0m, height 2.25m and length 5.75m. The model was mounted on the test section floor with a 'peniche' of 30mm thickness between the (half) fuselage and the floor (Fig. 3).

Acoustic array
The acoustic array in the tunnel side wall was situated at the pressure side of the wing. The 96 array microphones were mounted flush in the red support plate (Fig. 1), within a surface of 57 cm × 44 cm. In order to reduce the effect of interfering reflections and tunnel noise, the tunnel wall opposite to the array was fitted with a sound absorbing lining.
From the stored time domain data of the 96 microphones, the crosspower matrix has been calculated for a frequency resolution of 113 Hz and a maximum frequency of 58 kHz. Using a Hanning window and 50% overlap, a maximum of 4536 averages was possible for the applied measuring time of 20 seconds. Because of this large number of averages, the pressure fluctuations, caused by the unsteady flow in the turbulent boundary layer, are effectively suppressed. Therefore, a porous surface layer on top of the microphones[8,9], is not needed anymore. For the measurements (without flow) on the reference source, the measuring time was 2 seconds.
Using a conventional beamforming technique[8], a set of monopole sound power values have been calculated from the crosspower matrix, on a grid with a spacing of 2 cm. Finally, the 1/3-octave band source strengths, in terms of the sound power levels re 1 pW, have been determined from the corresponding narrow band data. The range of 1/3 octave bands covered by the measurements was from 50 kHz down to about 4 kHz.

Reference source
Fig. 2 shows the reference source which has been applied, and which is similar to the one described by Verheij et al[12]. The nozzle geometry is shown in Fig. 6. In the following, the position of the reference source is defined as the position of the mouth of the nozzle, which is shown in the detail picture in Fig. 2, see also Fig. 6. For low frequencies, the sound radiation of the nozzle is identical to that of a monopole, the upper frequency f_{max} of the "monopole frequency band" following from $ka \approx 0.5$, with k the wavenumber and a the nozzle radius. For the present nozzle (a = 3.5mm) the upper frequency is approximately $f_{max} \approx 7.7$ kHz.

Below the upper frequency f_{max}, the free field sound pressure $p(r)$ at a distance r from the source can easily be determined from the sound pressure p_N, measured by the reference microphone inside the nozzle[12,13]:

$$|p(r)| = \frac{S \times k \times |p_N|}{4\pi \times r \times \sin k(\Delta + 0.6 \times a)} \quad , \qquad (1)$$

in which $S = \pi a^2$ is the cross sectional nozzle surface, k the wavenumber and Δ = 10.4mm the distance between the reference microphone and the mouth of the nozzle, see Fig. 6.

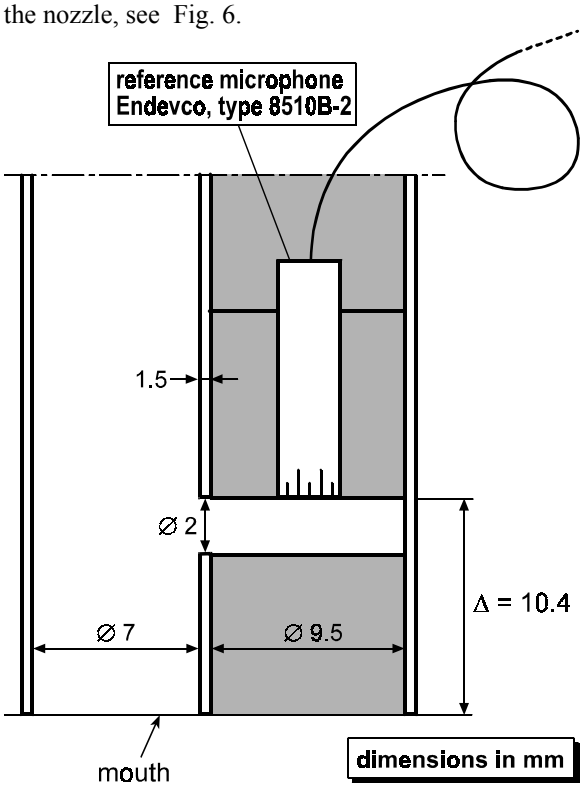

Fig. 6 Details of the reference source nozzle geometry

The ratio of the sound pressure amplitudes $|p(r)/p_N|$, in dB, is plotted in Fig. 7 for r = 1m (see legend, "theory"), together with data in 1/3 octave bands, measured in an anechoic room. It is observed that the measured data begin to deviate from the theory already at 2.5 kHz, i.e. for frequencies much lower than the upper frequency f_{max}. This is attributed to fact that the reference microphone happens to be mounted in a Helmholtzresonator, as can be seen in Fig. 6. In section 10.5 of Ref.[13], the effect of such a Helmholtzresonator on the sound pressure amplitude $|p(r)|$ is expressed as follows:

$$|p_H(r)| = |p(r)| \times \sqrt{\frac{R^2 + X^2}{(0.5 + R)^2 + X^2}} \, , \qquad (2)$$

with $p_H(r)$ the sound pressure at a distance r from the source, taking the Helmholtzresonator into account as a sidebranch of the tube, and R and X the normalized specific acoustic resistance and reactance (dimensionless) at the entrance of the side branch, with reference to the neck cross sectional surface S_n of the Helmholtzresonator. Expressions for R and X can found in the literature ([14] and [13] respectively):

$$R = \frac{\sqrt{8\nu\omega}}{c}\left(1+\frac{L}{2a_n}\right), \tag{3}$$

$$X = \frac{\omega(L+1.7a_n)}{c} - \frac{c\times S_n}{\omega\times V}, \tag{4}$$

with $\nu = 1.51\cdot10^{-5}$ m^2/s the kinematic viscosity of air, ω the angular frequency, $c = 340$ m/s the speed of sound in air, a_n the neck radius, $S_n = \pi \cdot a_n^2$ the cross sectional neck surface, L the neck length and V the resonator volume. The geometry of the present Helmholtzresonator is depicted in Fig. 6: a_n = 1mm, L = 1.5mm and V = 142mm^3. Fig. 7 shows the sound pressure ratio $|p_H(r)/p_N|$, in dB, for r = 1m (see legend, "theory with Hhr"), according to these values.

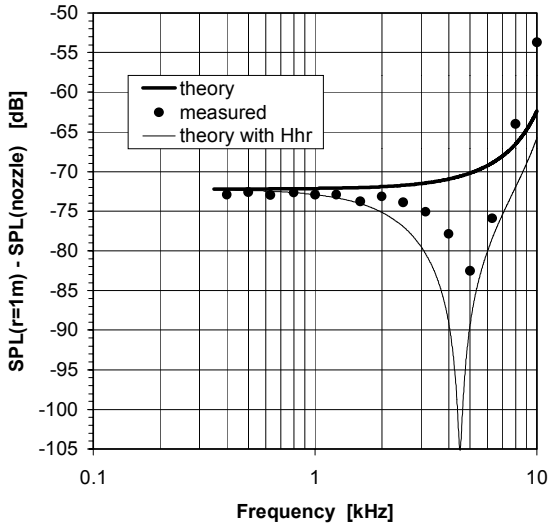

Fig. 7 Theoretical and measured differences between SPL data outside the reference source and inside the nozzle

The differences between the calculated $|p_H(r)/p_N|$ values and the measured data are attributed to inaccurate Helmholtzresonator modelling, in particular with respect to the resonator dimensions and the formula, used for the neck resistance, which includes probably not all effects, contributing to the actual neck resistance. Also the assumption that only the sound pressure $p(r)$, and not the sound pressure $p_N(r)$ is affected by the presence of the Helmholtzresonator, might be incorrect. Nevertheless, it is believed, that the measured data are accurate up to about the 8 kHz 1/3 octave band. Therefore, these data will be used as a reference ("calibration data") in the discussion of the experimental results, measured with the reference source.

Test conditions and measuring program

For all acoustic measurements, the model was placed on the tunnel axis. The axial position x and height z of the array microphones and the model are depicted in Fig. 8 (tunnel floor at z = –1.125m).

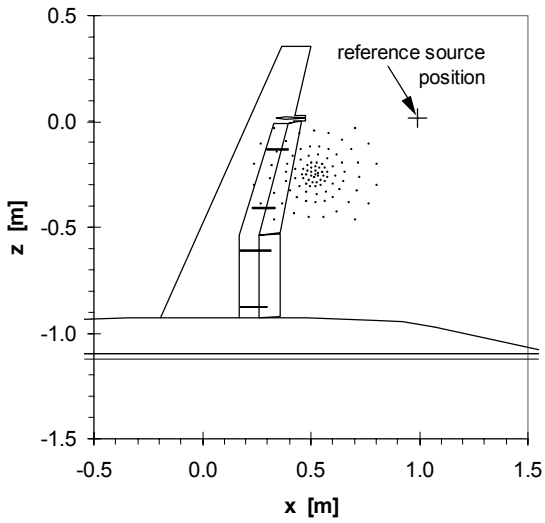

Fig. 8 Positions (only x- and z-coordinates) of aircraft model, array microphones and reference source

Measurements have been performed at two tunnel speeds:

- 60 m/s, corresponding with a Mach number of 0.18 and a Reynolds number based on the mean aerodynamic chord of about 1.4*10^6,
- 75 m/s, corresponding with a Mach number of 0.226 and a Reynolds number based on the mean aerodynamic chord of about 1.7*10^6.

In all cases the boundary layer on the wing as well as on the fuselage nose was tripped. On the wing this was achieved by means of 'zig-zag' tape at 3% to 4.5% of the local chord (Fig. 3). No tripping was applied to the fences. The acoustic tests on the landing configurations were performed for an angle of attack of 0.12° and a flap angle of 35°, representative for approach and landing, and corresponding with $C_L = 0.6\ C_{Lmax}$.

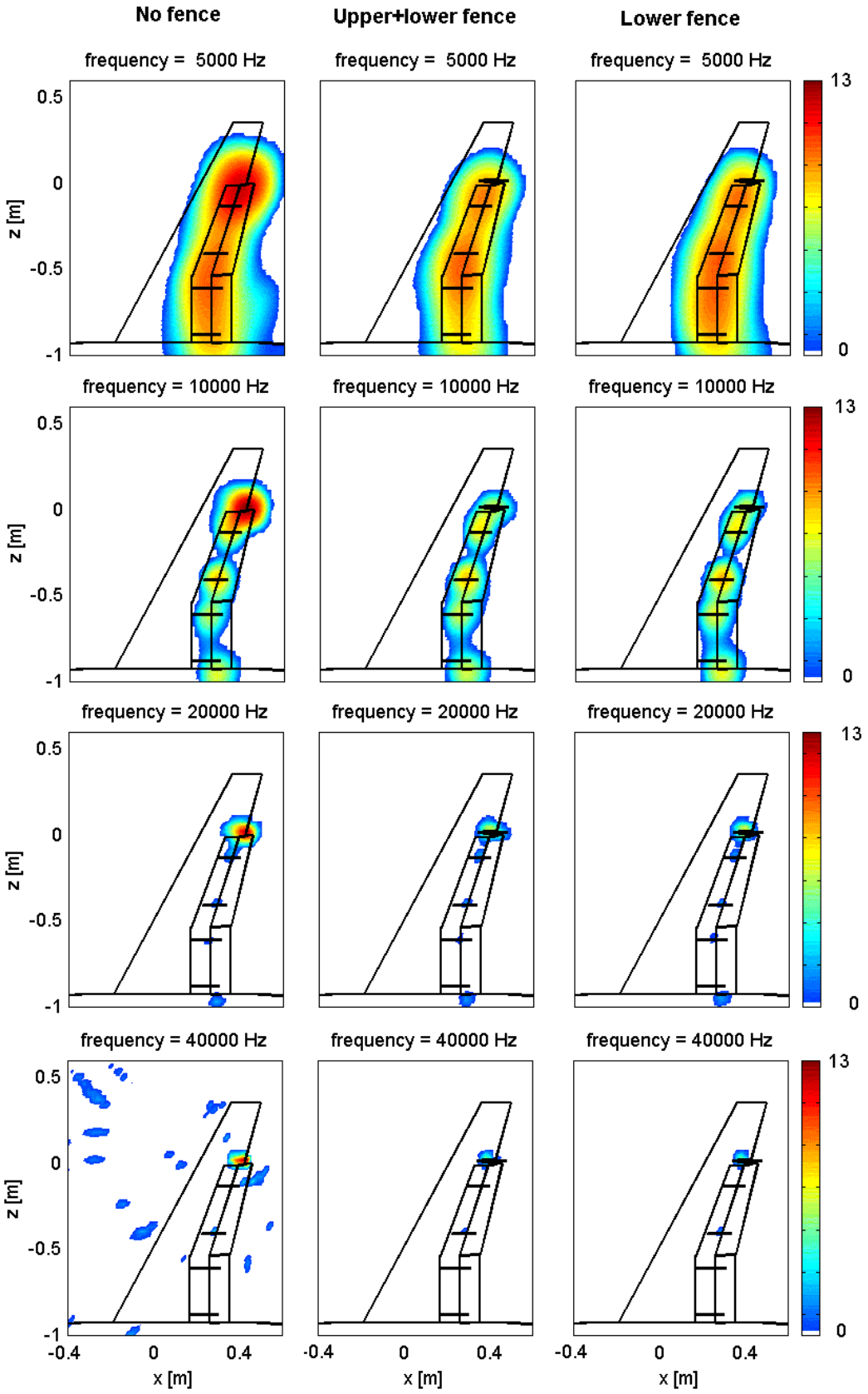

Fig. 9 Acoustic source plots of an aircraft wing at 75 m/s tunnel speed, for three configurations and four 1/3 octave bands; the dynamic range is 13 dB

Unless stated differently, the tests have been carried out with an absorbing tunnel wall opposite to the array. The following configurations have been tested:

1. reference ("clean") landing configuration,
2. same configuration as 1, but fitted with both an upper and a lower flap tip fence,
3. same configuration as 1, but fitted with only a lower flap tip fence,
4. same configuration as 1, but with a blunt trailing edge,
5. cruise configuration (as indication of the background noise; angle of attack 1.8° instead of 0.12°),
6. same configuration as 4, but with a reflecting instead of an absorbing tunnel wall opposite to the array.

The axial position x and height z of the reference source is indicated in Fig. 8. Two lateral positions have been applied: at $y = 0$ (this is the tunnel axis) and at $y = -1$m (which is 0.5m from the wall opposite to the array.

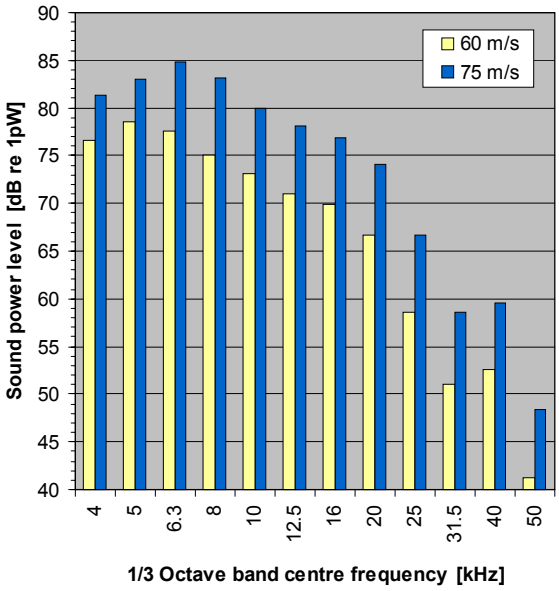

Fig. 10 Sound power level spectrum of flap tip source for two tunnel speeds

From earlier wind tunnel measurements with a half open test section[15] a significant decrease was found in the difference between measured and true source powers, after lining of the two test section walls with a sound absorbing lining. From computer simulations it appeared, that also in closed wind tunnels sound absorbing tunnel wall lining may have beneficial effects. For the test section of the DNW-LST the differences (in dB) between measured and true sound powers could decrease with 50%, after fitting the wall opposite to the array with a sound absorbing lining.

To investigate this further, the measurements on one of the aircraft model configurations and the measurements with the reference source have been executed both with a reflecting and an absorbing wall opposite to the array. The sound absorbing lining with a length of 4.73m was made up of 5cm sound absorbing foam, covered with a perforated plate.

III. Experimental results

Aircraft model

The main results of the acoustic measurements on the aircraft model are presented in Fig. 9 to Fig. 12.

First of all it is recalled that the used acoustic array technique allows the quantification of the noise sources on the wing under the assumption that the noise sources are of the monopole type, i.e. directivity is not accounted for. Fig. 9 presents a comparison of the noise source distributions as determined for the approach/landing configurations with and without the flap tip fences. Presented is the noise source distribution on the model for the 1/3 octave bands of 5, 10, 20 and 40 kHz at a tunnel speed of 75 m/s, over the scan plane $-0.4\text{m} \le x \le +0.6\text{m}$ and $-1.0\text{m} \le z \le +0.6\text{m}$. The (local) noise source distribution is given in terms of the sound power levels, expressed in decibels re 1 pW.

Fig. 9 illustrates clearly that for the "clean" configuration, that is without flap tip fences, the dominant noise source is located near the tip of the flap, over a broad range of frequencies. Two or three other, weaker sources appear to be associated with other sources, such as the flap brackets of the wind tunnel model, compare also Fig. 1 and Fig. 3.

The results also show a significant reduction of the strength of the dominant noise source for all presented 1/3 octave bands, in the order of 5 dB. This applies for both the lower-fence-only an the lower-plus-upper fence configuration. This suggests that only the lower fence has an important effect on airframe noise.

For the "clean" configuration, the source near the flap tip appeared to be the dominating noise source over the frequency range from about 5 to 50 kHz. The sound power levels of this source are plotted in Fig. 10 for the 1/3 octave bands from 4 to 50 kHz, for both tunnel speeds of 60 m/s and 75 m/s. Fig. 11 presents the sound power level reduction caused by the application of the flap tip fences as a function of frequency for two wind tunnel speeds (60 and 75 m/s). For each 1/3 octave band, the sound power level (reduction) in Fig. 10 (Fig. 11) is assumed to be equal to (the reduction of) the maximum sound power

level in the domain $0.23\ m \le x \le 0.43\ m$ and $-0.1\ m \le z \le 0.1\ m$ around the flap tip (see Fig. 8 and Fig. 9).

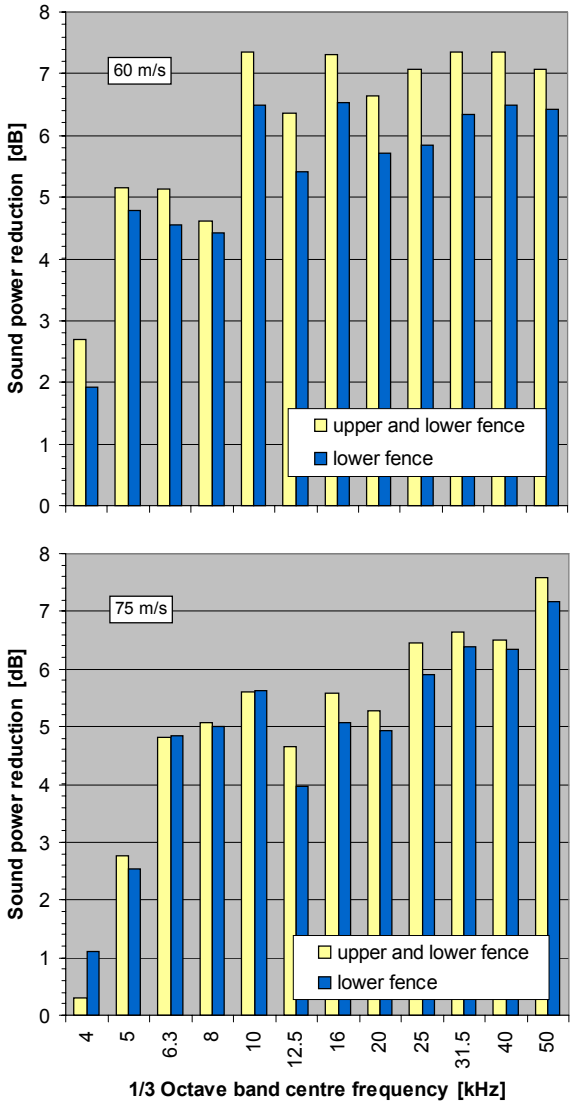

Fig. 11 Noise reduction spectra of flap tip source for both fence configurations and two tunnel speeds

From Fig. 11 it appears that

- the fences are most effective for frequencies above about 6 kHz (model scale),
- for 60 m/s the noise source reduction (up to about 7 dB) of the lower-plus-upper fence configuration is slightly larger than the reduction (up to about 6 dB) of the lower-fence-only configuration,
- for 75 m/s the difference between the two fence configurations is insignificant.

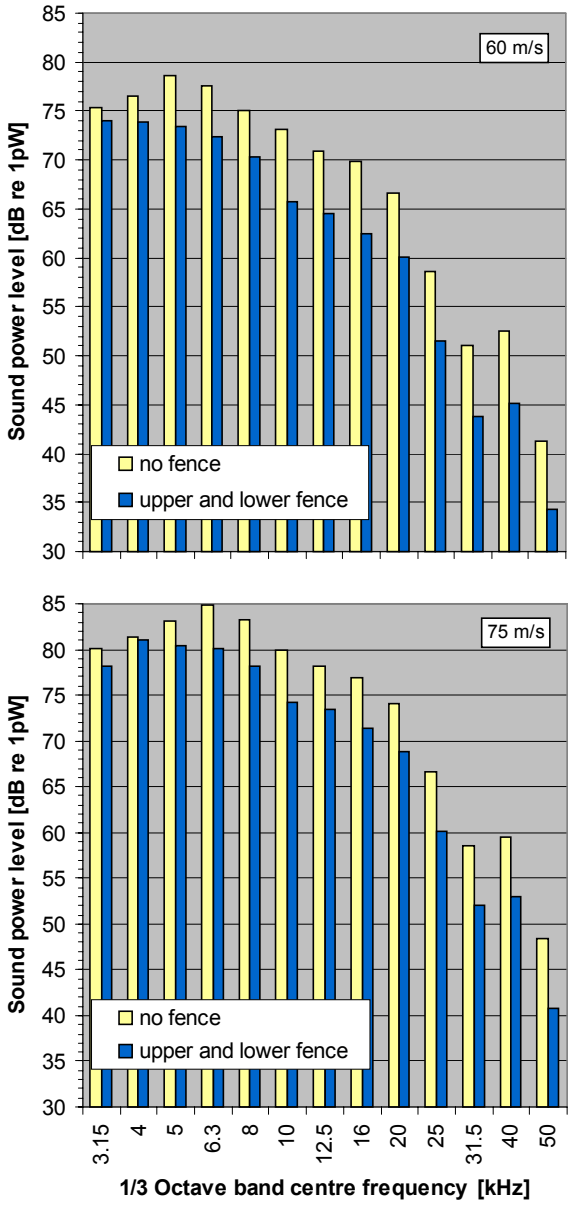

Fig. 12 Sound power level spectra of flap tip source for two tunnel speeds, without and with flap tip fence

Fig. 12 shows the sound power level spectrum of the flap tip source, without and with (upper plus lower) fence, for both applied tunnel speeds. Besides a sound power reduction, the fence causes also a decrease of the "peak"frequency (i.e. the frequency for which the maximum sound power is emitted), as can be observed in Fig. 12. For the configuration with only the lower fence, the same frequency shift was found. The same effect has been reported by Guo[6], however measured on surface pressure spectra. Upscaling from model scale (8.5% in the present case) to full scale, the decreased peakfrequency will be well below 1 kHz in most cases. Then, this frequency shift leads

to an extra reduction of the total (broadband) sound power level in dB(A) and the corresponding EPNdB levels.

For the configuration with a blunt trailing edge, the source strengths of the dominant (flap tip) noise source were about equal to those of the reference configuration (average (maximum) increase of 0.5 (2) dB, over the 4-50 kHz 1/3 octave bands). In order to investigate the possible appearance of sources on the trailing edge, the flap tip source strength has been reduced by more than 10 dB with a principal component technique[16]. However, no significant sources on the trailing edge were found.

For the cruise configuration the maximum sound power levels in the scan plane were 10 to 20 dB below the maximum values for the reference landing configuration, over the 4-50 kHz frequency range. The true source strength differences between cruise and landing configuration are still higher, as the most significant "sources" for the cruise configuration were located outside the aircraft model. The source strengths, measured on the cruise configuration may thus be regarded as a measure for the wind tunnel background noise.

All model configurations have been tested with a sound absorbing tunnel wall opposite to the array. The blunt trailing edge configuration has also been tested with a reflecting tunnel wall. For the reflecting wall, the maximum sound power levels in the scan plane were higher than for the absorbing wall. For the 1 kHz 1/3 octave band the difference was about 5 dB, decreasing to less than 0.5 dB for the 5-50 kHz 1/3 octave bands. For both tunnel speeds the differences were approximately the same. These results agree with the anticipation that tunnel wall reflections become more important at low frequencies. It is noted that the spatial resolution of the present array (dimensions 57cm×44cm), for frequencies lower than about 4 kHz, is insufficient for reliable results. From this, it can be concluded that the effect of the sound absorbing wall on the results of the present model (which was located near the lateral tunnel axis, i.e. $y \approx 0$) is negligible. However for source positions close to the wall opposite to the array, an absorbing wall may have a significant effect, as will be shown below.

For the configuration with upper plus lower fence, an additional measurement has been carried out, the array being covered with 5mm foam and a perforated plate (5% open, thickness 0.45mm)[8]. For the 4 and 5 kHz 1/3 octave bands, the measured source strengths were about the same as for the measurement without foam. For higher frequencies the source strengths for the measurement with foam were systematically lower than for the measurement without foam, the difference increasing with frequency (10 dB at 25 kHz). Above 25 kHz the results of the measurement with foam were unusable, due to spurious sources outside the model.

Finally, the effect of the measuring time has been explored. An increase of the measuring time from 20 to 30 sec. yielded identical source power data. A decrease to 10 sec. caused a very small increase of the noise floor in the source strength plots.

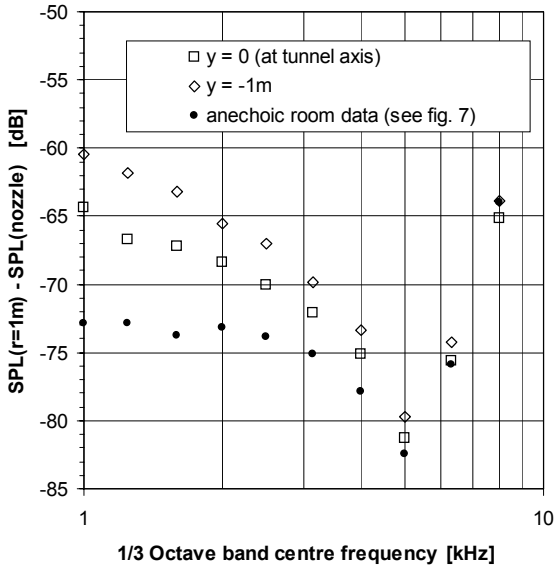

Fig. 13 Measured differences between SPL data outside the reference source and inside the nozzle, effect of tunnel wall distance

Reference source

The most important results of the measurements on the reference source are presented in Fig. 13 and Fig. 14. From the sound powers, determined from the array data, the free field sound pressure levels SPL(r=1m) at a distance of r = 1m from the reference source have been calculated. The test results on the reference source are expressed in terms of SPL differences SPL(r=1m) – SPL(nozzle), with SPL(nozzle) the sound pressure level, measured by the reference microphone in the nozzle, see Fig. 6. For the present measurements, this difference may be assumed to be independent of SPL(nozzle). In order to simplify the following discussion the sound pressure level SPL(nozzle) is set to zero (by definition), so that the level difference SPL(r=1m) – SPL(nozzle) may be interpreted as the sound pressure level SPL(r=1m). Fig. 13 and Fig. 14 show the SPL differences (interpreted as SPL(r=1m))

for two positions of the reference source ($y = 0$ and $y = -1$m, see Fig. 8 for the x- and z-coordinates of both source positions). As a reference, the "calibration data", measured in the anechoic room (Fig. 7) are also plotted. It is recalled that the upper frequency f_{max}, for which the sound radiation of the reference source is identical to that of a monopole, amounts approximately to $f_{max} \approx 7.7$ kHz. Therefore, the data in Fig. 13 and Fig. 14 are presented up to the 1/3 octave band of 8 kHz.

Fig. 13 shows the SPL(r=1m) data for the two reference source positions for the case of reflecting tunnel walls. For the source located at $y = 0$ (i.e. at the tunnel axis), the SPL(r=1m) levels for the 6.3 and 8 kHz 1/3 octave bands are almost equal to the corresponding levels, measured in the anechoic room. For lower frequencies, the SPL(r=1m) levels are higher than the corresponding levels, measured in the anechoic room, the difference increasing with decreasing frequency. For the source located at $y = -1$m (i.e. 0.5m from the wall opposite to the array), the SPL(r=1m) levels are systematically higher than for $y = 0$, the difference increasing with decreasing frequency. For the 6.3 and 8 kHz the SPL(r=1m) levels for $y = 0$ and $y = -1$m in Fig. 13 are about equal.

The SPL differences for $y = 0$ and $y = -1$m agree again with the anticipation of larger effects of tunnel wall reflections at lower frequencies. For the 1/3 octave bands of 6.3 and 8 kHz, the effects of tunnel wall reflections on the SPL(r=1m) levels appear to be very small. Furthermore, the effects of tunnel wall reflections increase, as expected, for source positions closer to the tunnel wall opposite to the array.

Fig. 14 shows the same data as Fig. 13, with added the corresponding data, measured with an absorbing tunnel wall opposite to the array. For the source located at $y = 0$, the SPL(r=1m) levels for the absorbing wall are only slightly lower than for the reflecting wall (maximum difference 1 dB for 1.25 kHz and higher 1/3 octave bands). For the source position $y = 0$, the effect of the absorbing wall on the measured source strengths appears to be about the same (4 kHz and higher 1/3 octave bands) or smaller (3.15 kHz and lower 1/3 octave bands) than for the aircraft model, tested with both the reflecting and absorbing tunnel wall (configurations 4 and 6). For the $y = -1$m source position, the SPL(r=1m) levels for the absorbing wall in Fig. 14 are at most 1 dB lower than for the reflecting wall, however only for the 4 kHz and higher 1/3 octave bands. For the lower 1/3 octave bands, the difference between the SPL(r=1m) levels for the reflecting and the absorbing wall are gradually increasing up to 5 dB at 1 kHz
The effect of additional lining on the wind tunnel ceiling and floor (8cm sound absorbing foam with a length of about 5m) on the SPL(r=1m) levels was smaller than 1 dB, for the 1/3 octave bands from 1 to 8 kHz.

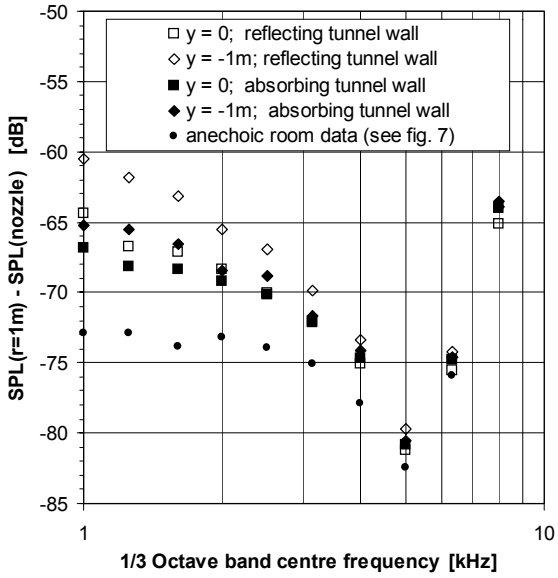

Fig. 14 Measured differences between SPL data outside the reference source and inside the nozzle, effect of absorbing tunnel wall

The data in Fig. 14 support the conclusion that (at least for monopole sources near the tunnel axis) an absorbing tunnel wall has little effect on the source strengths, measured with an array with the present dimensions. Bearing in mind that the spatial resolution of the present array is sufficient for frequencies of about 4 kHz and higher, the same conclusion holds for source positions more close to the tunnel wall. For a larger array however, an absorbing tunnel wall might be more beneficial, in particular for sound sources near the wall opposite to the array.
Once more, it is recalled that these conclusions are valid only for sound sources with a monopole like radiation pattern, i.e. sources without a pronounced directivity.

IV. Conclusions

Exploratory, low-speed wind tunnel tests have been performed on a 8.5% half model in landing configuration, to investigate the (aerodynamic and) aero-acoustic effects of "flap tip fences", mounted at the position of the outboard tip of the trailing-edge flap, and a blunt flap trailing edge.
Two winglet type "fence" configurations have been

investigated: a single one extending downward (and rearward) from the lower surface of the wing and a double one extending upward as well as downward from the wing. The blunt flap trailing edge was about three times as thick as the standard trailing edge.
The main results with respect to the aero-acoustic effects are:

- A substantial (up to 7 dB) reduction of the source strength of the flap tip (about equal for the lower and the upper plus lower fence configurations).
- A decrease of the frequency, for which the maximum sound power is emitted (about equal for the lower and the upper plus lower fence configurations). This frequency shift leads to an extra reduction of the total (broadband) full scale sound power level in dB(A).
- No significant aero-acoustic effects were found for the blunt trailing edge.

For the 5-50 kHz frequency band, equal sound power levels in the scan plane were found both for the reflecting and for the absorbing tunnel wall opposite to the array (blunt trailing edge configuration). This was found for both tunnel speeds.

To obtain an impression of the differences between the measured and true values of the acoustic source strengths, and the effect of absorbing tunnel walls on these differences, also measurements have been carried out with a reference source, with a known volume velocity. The most important results of these measurements are:

- For both source locations ($y = 0$ and $y = -1$m), the sound powers for the 6.3 and 8 kHz 1/3 octave bands were almost equal to the corresponding levels, measured in the anechoic room.
- An absorbing tunnel wall opposite to the array had little effect on the source strengths, measured by the acoustic array.

The most important conclusions, which can be drawn from these results are:

- Flap tip fences can provide a significant reduction (more than 5 dB) of flap side-edge noise, over a broad frequency range.
- For the present set-up, and for the 6.3 and 8 kHz 1/3 octave bands, the errors in the acoustic source strengths due to tunnel wall reflections are small. This conclusion is expected to hold also for higher frequencies.

These conclusions are valid only for sound sources with a monopole like radiation pattern, i.e. sources without a pronounced directivity.

References

[1] J.A. Hayes, W.C. Horne, P.T. Soderman, P.H. Bent, “Airframe noise characteristics of a 4.7% scale DC-10 model”, AIAA Paper 97-1594, 1997.

[2] Guo, Y.P., “Modeling of noise reduction by flap side edge fences”, AIAA Paper 00-2065, 2000.

[3] Brooks, T.F., Humphreys Jr., W.M., “Flap edge aeroacoustic measurements and predictions”, AIAA Paper 2000-1975, 2000.

[4] Revell, J.D., Kuntz, H.L., Balena, F.J., Horne, C., Storms, B.L., Dougherty, R.P., “Trailing-edge flap noise reduction by porous acoustic treatment”, AIAA Paper 97-1646-CP, 1997.

[5] Storms, B.L., Hayes, J.A., Jaeger, S.M., Soderman, P.T., “Aeroacoustic study of flap-tip noise reduction using continuous moldline technology”, AIAA Paper 2000-1976, 2000.

[6] Guo, Y.P., Joshi, M.C., Bent, P.H., Yamamoto, K.J., “Surface pressure fluctuations on aircraft flaps and their correlation with far-field noise”, Journal of Fluid Mechanics, vol. 415, pp. 175-202. 2000.

[7] Storms, B.L., Hayes, J.A., Moriarty, P.J., Ross, J.C., “Aeroacoustic measurements of slat noise on a three-dimensional high-lift system”, AIAA Paper 99-1957, 1999.

[8] Sijtsma , P., Holthusen, H., “Source location by phased array measurements in closed wind tunnel sections”, AIAA Paper 99-1814, 1999.

[9] Jaeger, S.M., Horne, W.C., Allen, C.S., “Effect of surface treatment on array microphone self-noise”, AIAA Paper 2000-1937, 2000.

[10] Holthusen, H., and Smit, H., “A new data acquisition system for microphone array measurements in wind tunnels”, AIAA paper 2001-2169, 2001.

[11] Slooff, J.W., de Wolf, W.B., Van der Wal, H.M.M., “Aerodynamic and aero-acoustic effects of flap tip devices”, NLR-TR-2000-476, 2000.

[12] Verheij, J.W., van Tol, F.H., Hopmans, L.J.M., “Monopole airborne sound source with in situ measurements of its volume velocity”, Proceedings Inter Noise 1995, pp. 1105-1108.

[13] Kinsler, L.E., Frey, A.R., Coppens, A.B., Sanders, J.V., “Fundamentals of Acoustics”, John Wiley, 3rd edition, 1982.

[14] Guess, A.W., “Calculation of perforated plate liner parameters from specified acoustic resistance and reactance”, Journal of Sound and Vibration 40(1), pp. 119-137, 1975.

[15] Oerlemans, S., and Sijtsma, P., “Effects of wind tunnel side-plates on airframe noise measurements with phased arrays”, AIAA Paper 2000-1938, 2000.

[16] Leuridan, J., Roesems, D, Otte, D., ”Use of Principal Component Analysis for correlation analysis between vibration and acoustical signals”, Proceedings of the 16th International Symposium on Automotive Technology and Automation (ISATA), Florence (Italy), 1987, pp. 487-504.